Supplemental Data. Falque et al. (2009). Two Types of Meiotic Crossovers Coexist in Maize

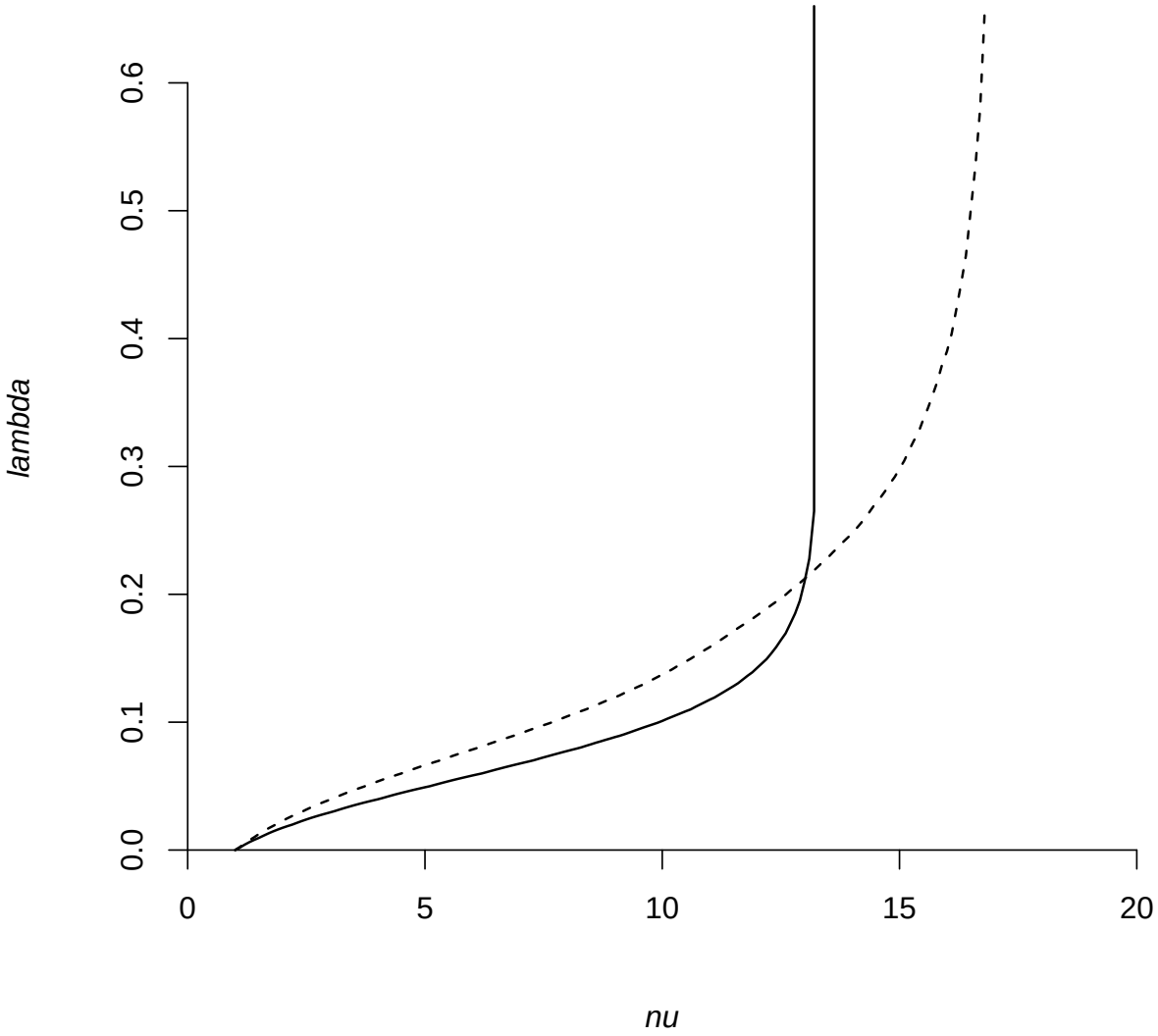

Supplemental Figure 1. Correspondence between interference strength parameters in the gamma and BF models.

X-axis: interference strength parameter ν of the gamma model. Y-axis: interference strength parameter λ of the BF model. Both models are single-pathway (no sprinkling). Case of maize chromosomes 1 (solid line) and 10 (dashed line).

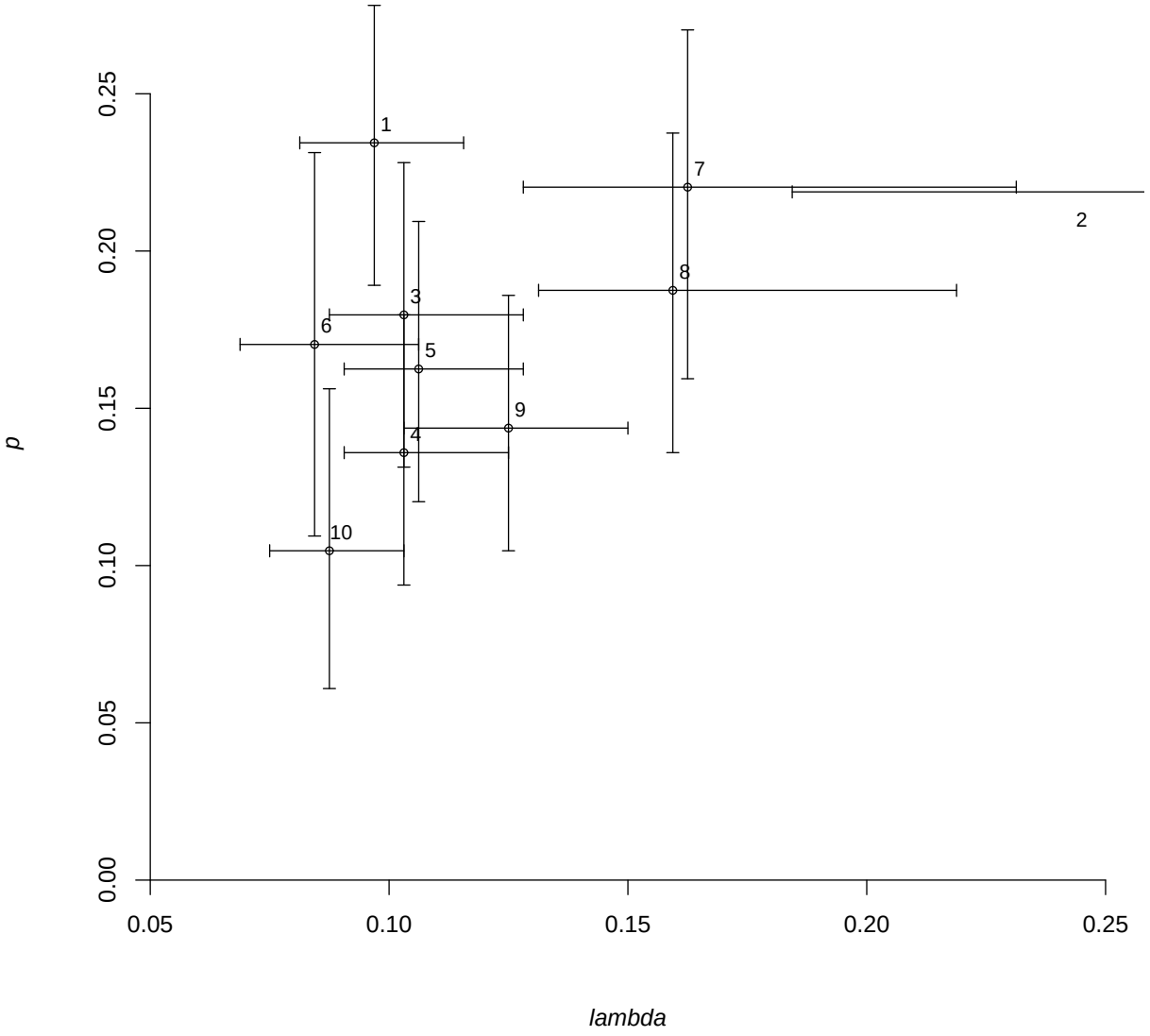

Supplemental Figure 2. Interference intensity and proportion of non-interfering COs using the BFS model.

Estimated values of the interference intensity of Pathway 1 (λ) and proportion of Pathway 2 COs (p), obtained by fitting the BFS model to maize LN data for each chromosome. The PLS score was used to fit the model. Horizontal and vertical bars indicate 95% confidence intervals (CI) based on 1000 simulated data sets. For chromosome 2, $p = 0.22$ but no finite estimate of λ could be obtained.

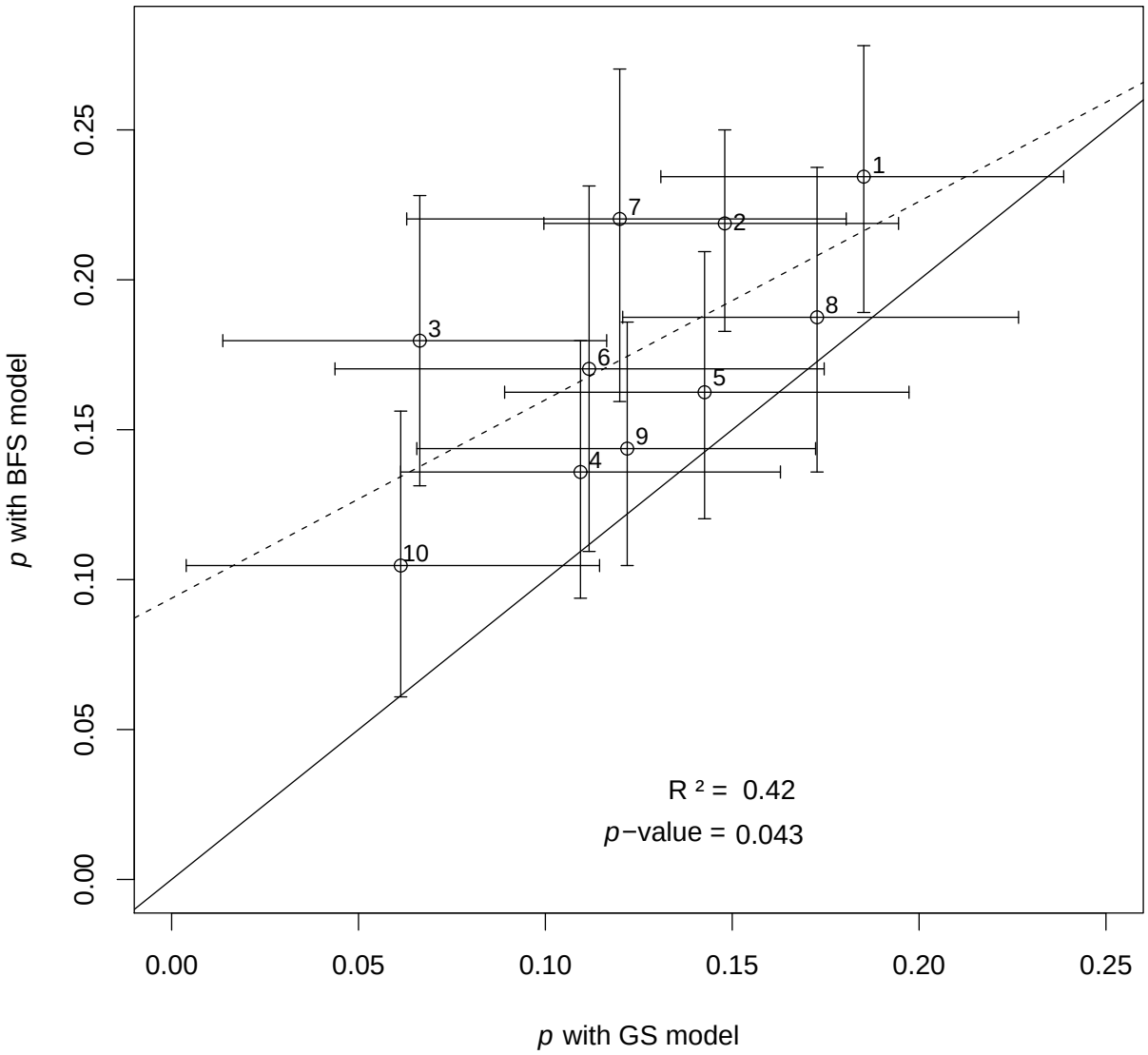

Supplemental Figure 3. Comparison of the fractions of non-interfering COs obtained with the GS and the BFS models.

Correlation between estimates obtained using GS and BFS models, for the proportion *p* of COs generated through Pathway 2 (non-interfering). Error bars are 95% confidence intervals determined by re-simulation (see text). Solid line: first diagonal. Dashed line: regression. R^2 and *p*-value: correlation coefficient with its associated *p*-value.

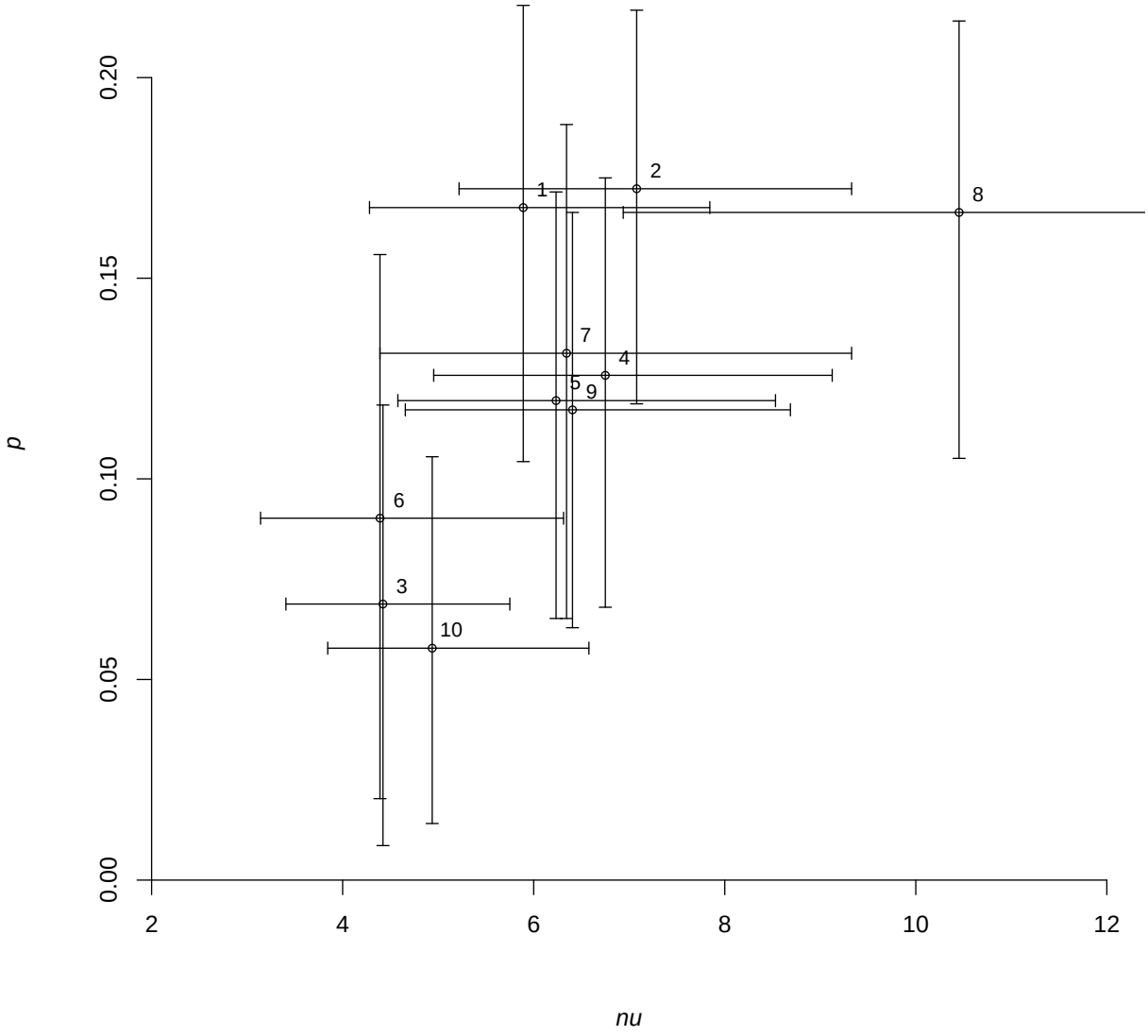

Supplemental Figure 4. Interference intensity and proportion of non-interfering COs with the GS model, using the PLS score for fitting.

Estimated values of the interference intensity (ν) in the Pathway 1 (interfering) and proportion of Pathway 2 (non-interfering) COs (p), obtained by fitting the GS model to maize LN data using the PLS score for each chromosome. Horizontal and vertical bars indicate 95% confidence intervals (CI) based on 1000 simulated data sets. For chromosome 8 the upper bound of the CI on ν is 15.3.

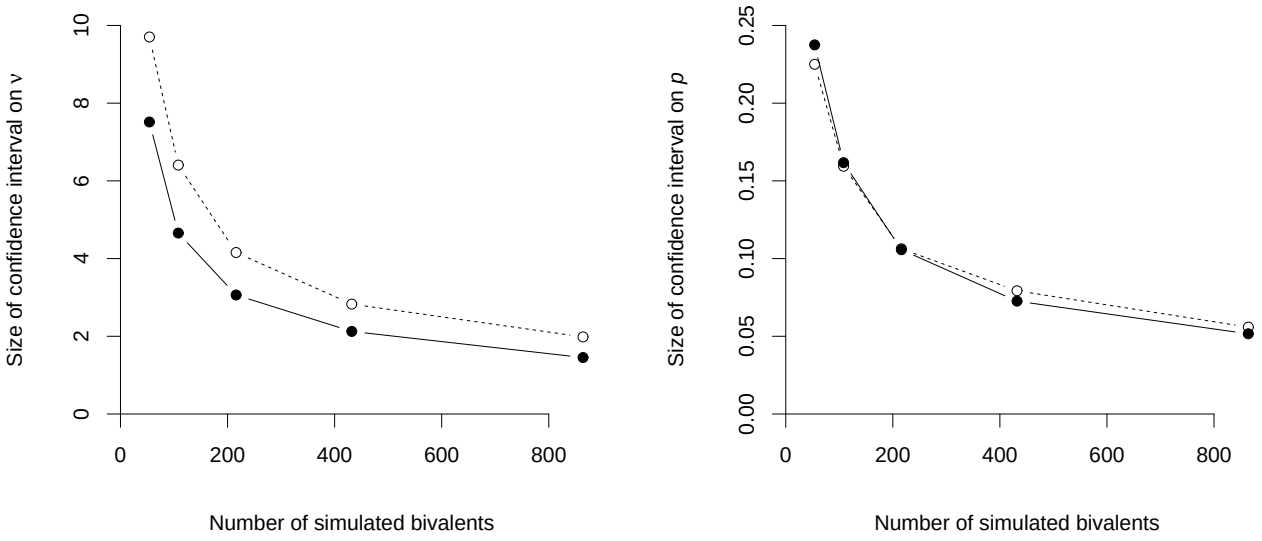

Supplemental Figure 5. Comparison of the fitting power obtained when using the PLS score or the full likelihood.

Power (given by the size of the confidence interval) of the fitting procedure as a function of the number of SCs in the data set. Left panel: case of the interference strength ν. Right panel: case of the proportion p of Pathway 2 COs. Solid lines and symbols are for estimates using maximum likelihood in the GS model. Dashed lines and open symbols are for estimates using the PLS score, also in the GS model. Confidence intervals were obtained as described in the Methods section of the article, from 10^3 independent simulated data sets; the value of p and ν used to generate these data sets were those obtained from the fits of chromosome 1. X-axis: number of simulated SCs in each of the 10^3 simulated data sets.

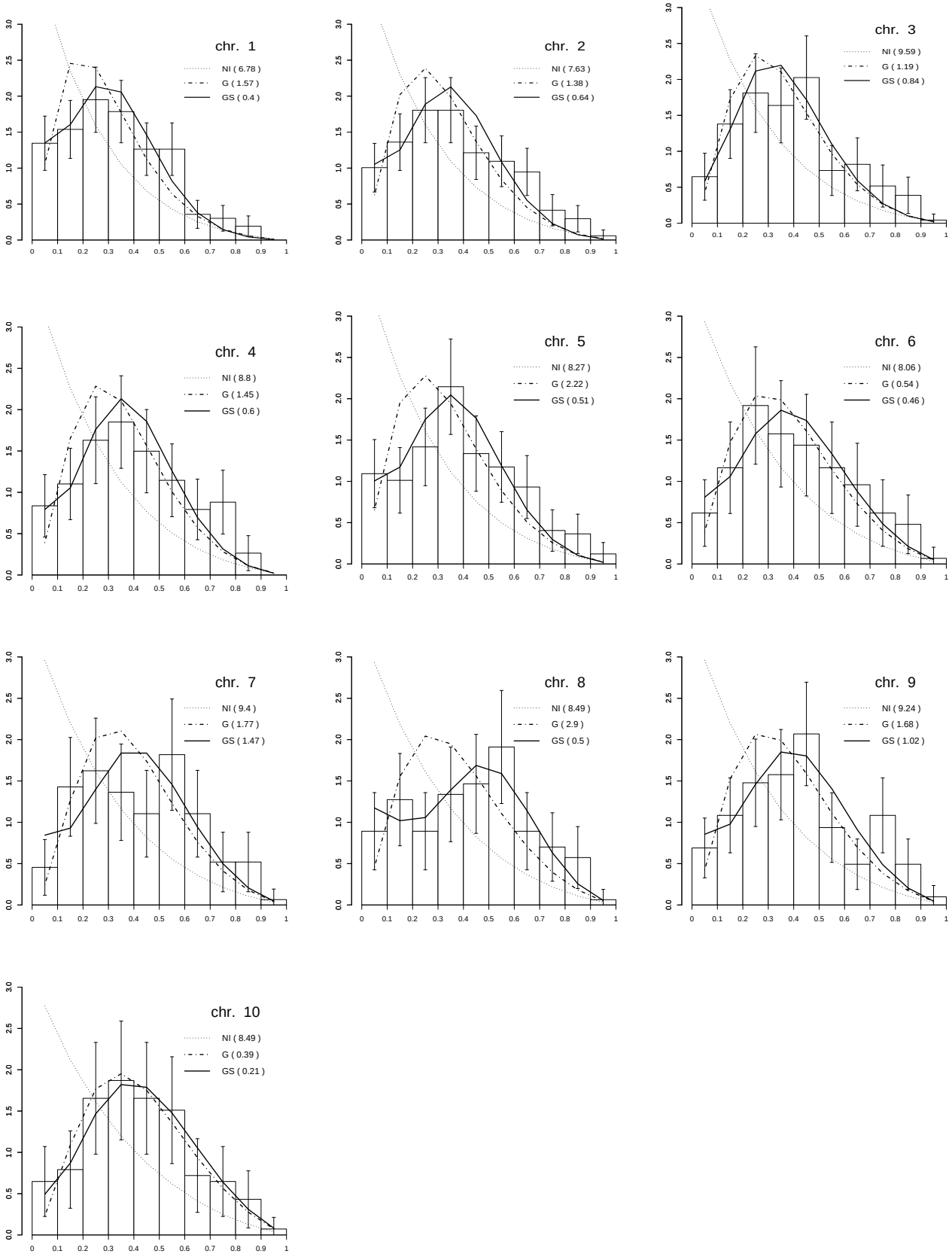
chr. 1
NI (6.78)
G (1.57)
GS (0.4)
chr. 2
NI (7.63)
G (1.38)
GS (0.64)
chr. 3
NI (9.59)
G (1.19)
GS (0.84)
chr. 4
NI (8.8)
G (1.45)
GS (0.6)
chr. 5
NI (8.27)
G (2.22)
GS (0.51)
chr. 6
NI (8.06)
G (0.54)
GS (0.46)
chr. 7
NI (9.4)
G (1.77)
GS (1.47)
chr. 8
NI (8.49)
G (2.9)
GS (0.5)
chr. 9
NI (9.24)
G (1.68)
GS (1.02)
chr. 10
NI (8.49)
G (0.39)
GS (0.21)

Supplemental Figure 6. Quality of the fits obtained with single-pathway or two-pathways models (gamma model).

Density distribution of distances between adjacent LNs in all SCs with at least two LNs for all maize chromosomes. X-axis: relative genetic distance. Bars: experimental observations. Lines: simulations with No-Interference (NI), single-pathway gamma model (G), or two-pathways gamma-sprinkling model (GS). In parentheses: sum of squares of differences between experimental and simulated densities.

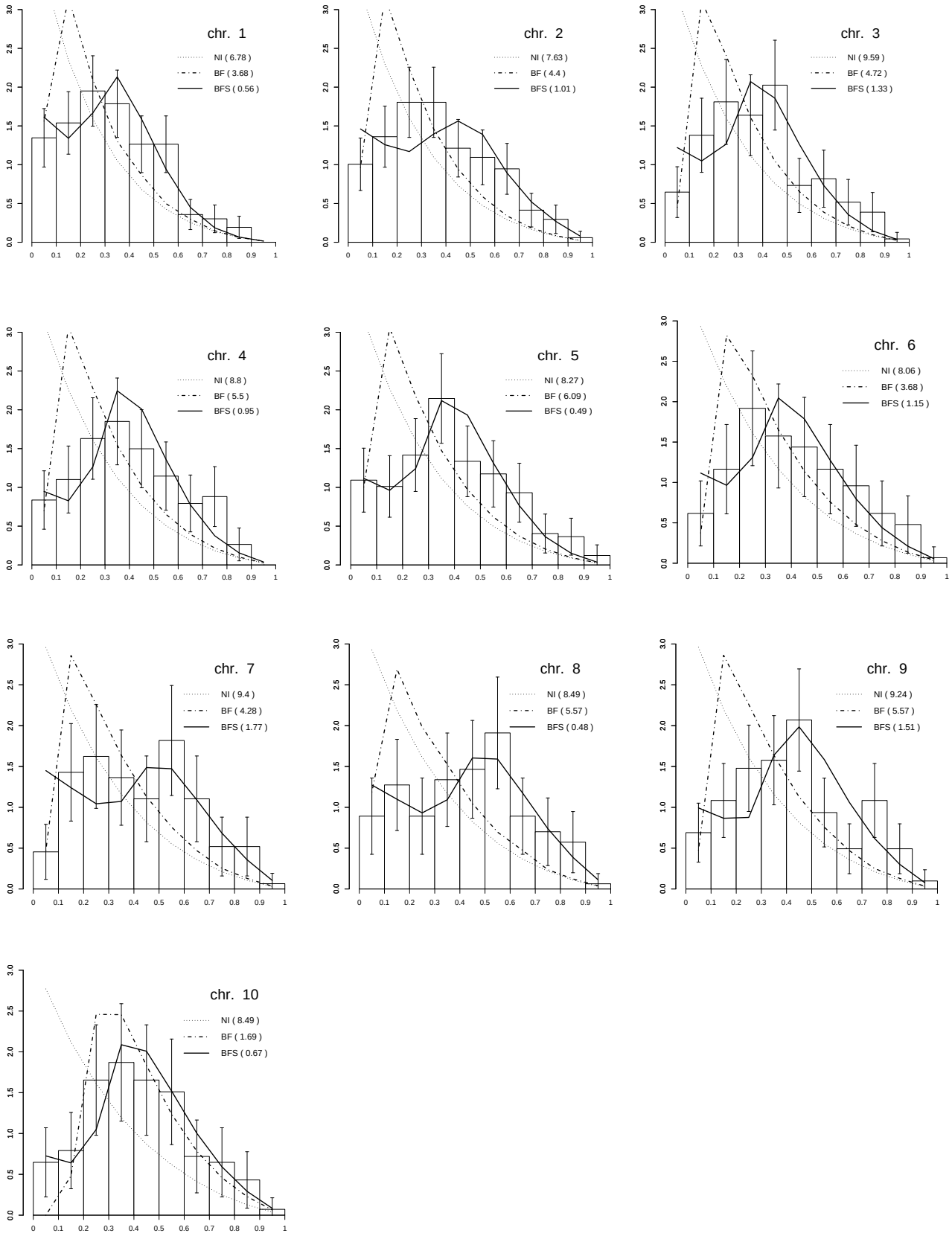
chr. 1
NI (6.78)
BF (3.68)
BFS (0.56)
chr. 2
NI (7.63)
BF (4.4)
BFS (1.01)
chr. 3
NI (9.59)
BF (4.72)
BFS (1.33)
chr. 4
NI (8.8)
BF (5.5)
BFS (0.95)
chr. 5
NI (8.27)
BF (6.09)
BFS (0.49)
chr. 6
NI (8.06)
BF (3.68)
BFS (1.15)
chr. 7
NI (9.4)
BF (4.28)
BFS (1.77)
chr. 8
NI (8.49)
BF (5.57)
BFS (0.48)
chr. 9
NI (9.24)
BF (5.57)
BFS (1.51)
chr. 10
NI (8.49)
BF (1.69)
BFS (0.67)

Supplemental Figure 7. Quality of the fits obtained with single-pathway or two-pathways models (beam-film model).

Density distribution of distances between adjacent LNs in all SCs with at least two LNs for all maize chromosomes. X-axis: relative genetic distance. Bars: experimental observations. Lines: simulations with No Interference (NI), single-pathway beam-film model (BF), or two-pathways beam-film sprinkling (BFS) model. In parentheses: sum of squares of differences between experimental and simulated densities.

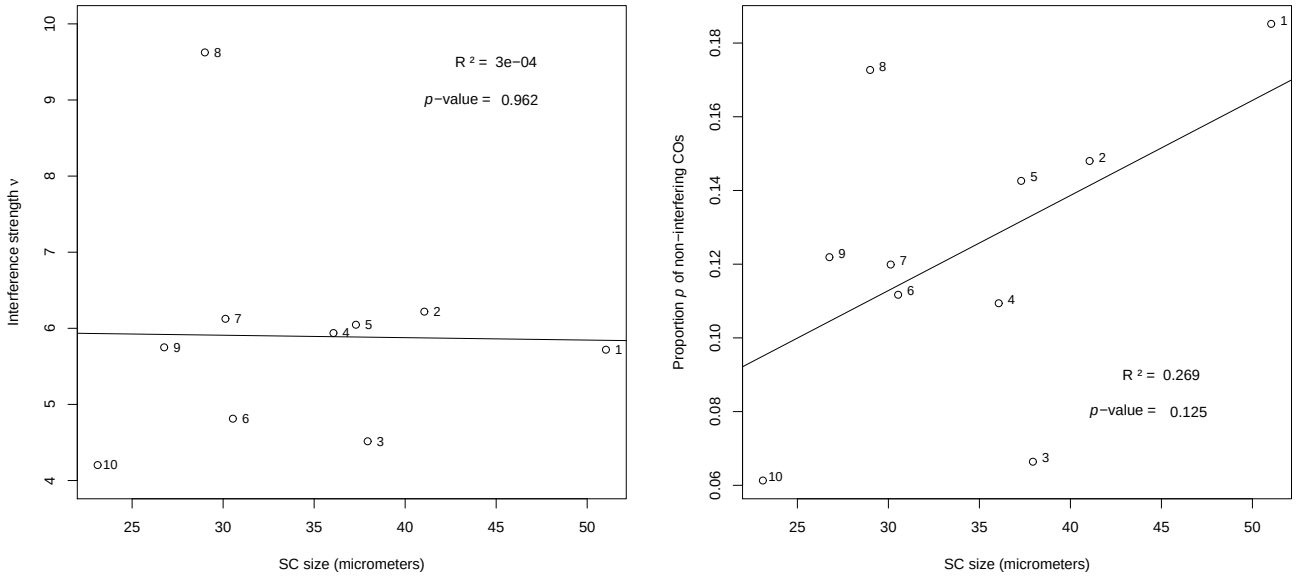

Supplemental Figure 8. Interference strength in Pathway 1 and fraction of non-interfering COs, as a function of SC length.

Correlation between the interference strength of Pathway 1 (ν, left panel), and proportion of Pathway 2 (non-interfering) COs (p, right panel), with the physical length of the SC across the ten maize chromosomes. Parameters have been estimated within the GS model.

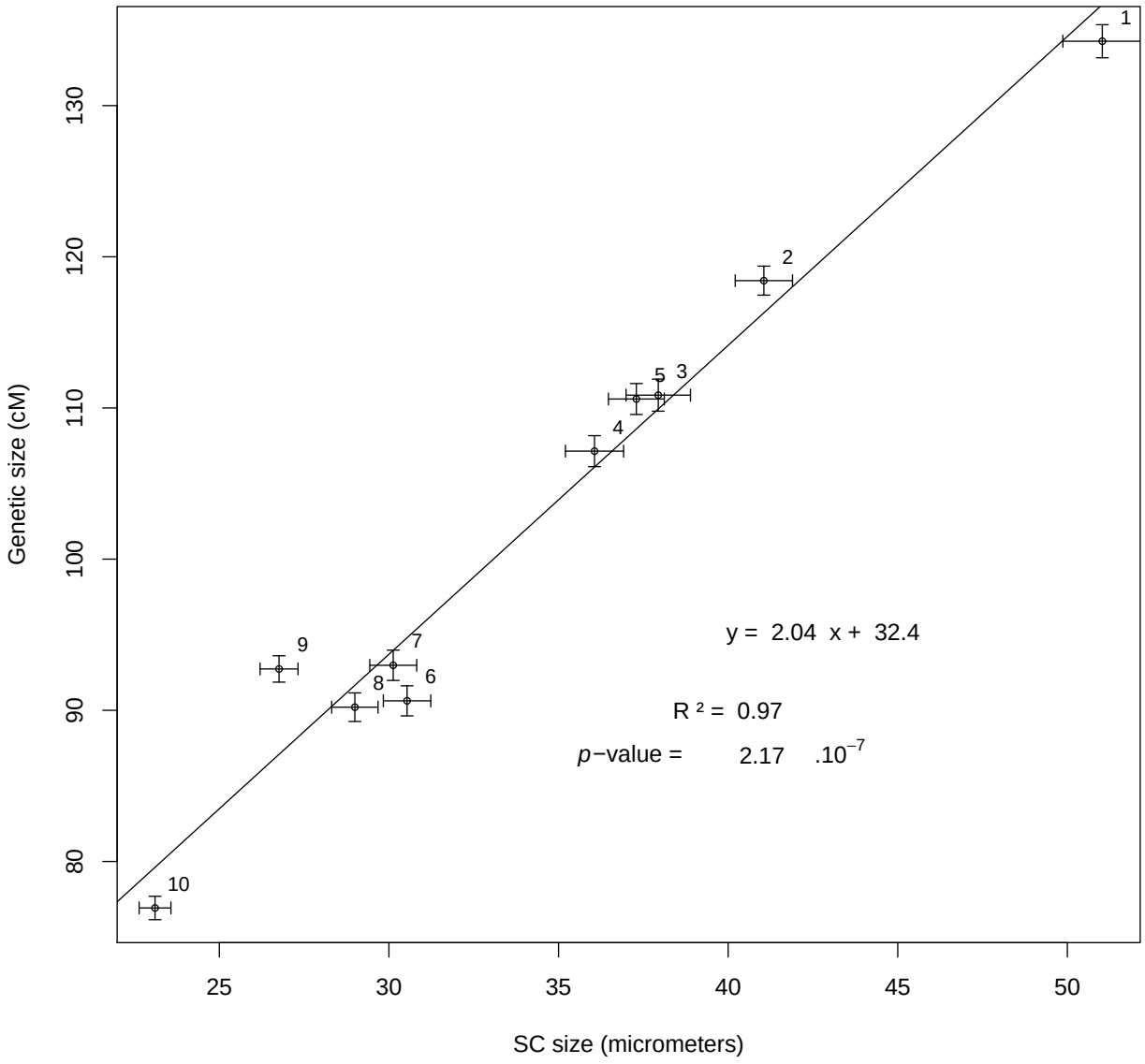

Supplemental Figure 9. Correlation between genetic and SC length across the 10 maize chromosomes.

Genetic length in centiMorgans is determined as 50 times the mean number of LNs per SC. Extrapolating the regression to small SC sizes leads to a genetic length of 32.4 cM.

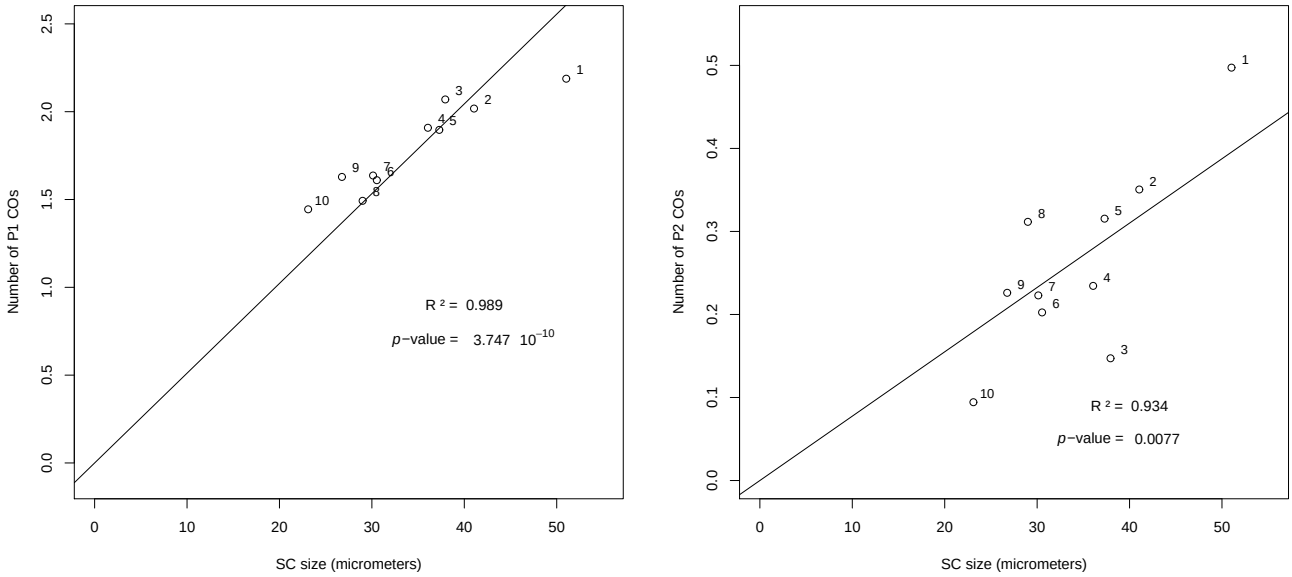

Supplemental Figure 10. Numbers of Pathway 1 and Pathway 2 COs as a function of SC length. Estimated mean numbers of COs formed through Pathway 1 (interfering; left panel), and through Pathway 2 (non-interfering; right panel) as a function of the SC length for the 10 maize chromosomes. R^2 is for the linear regression using model y=ax for both panels. The *p*-value is for the hypothesis of no association (constant *y*).

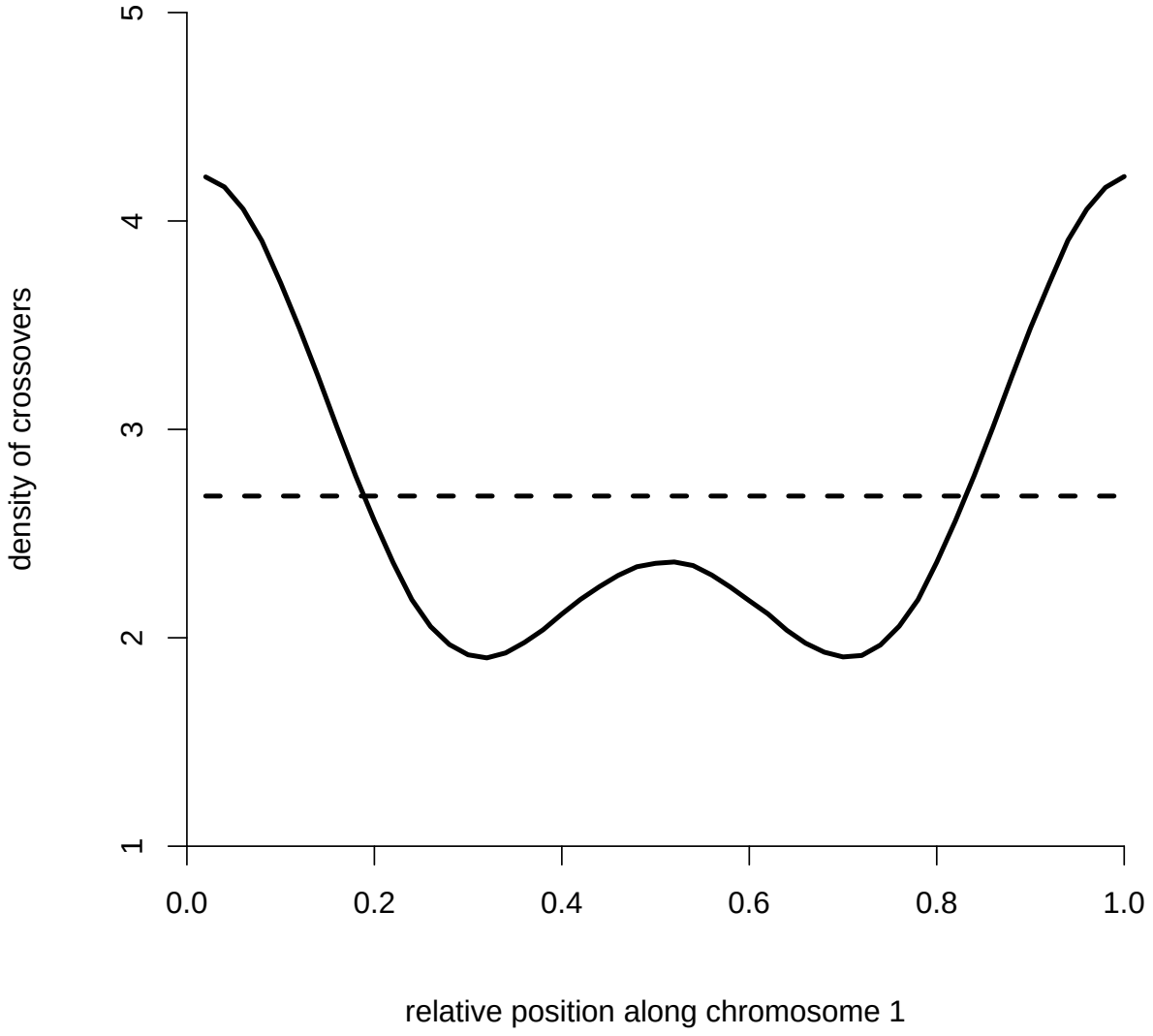

Supplemental Figure 11. CO density generated by the BF model.

Simulated CO density distribution as generated by the BF model in IRD space with λ = 0.2 (solid line), or by the gamma model in genetic space with any value for ν (dashed line). Chromosome size is that of maize chromosome 1 (genetic length = 134 cM).

Supplemental Methods. Specifications of the Models and Detailed Methods.

1. Interference models

In nearly all organisms, it has been found that crossovers (COs) do not arise independently. Typically, CO positions seem to be subject to a "repulsion" phenomenon whereby the frequency of obtaining two nearby COs is very small compared to what is expected if the COs were to form as independent events. For modeling such interference, we focus here on the gamma model (McPeek and Speed, 1995) which is the most frequently used SRP-based statistical model, and on the beam-film (BF) model (Kleckner et al., 2004) which is a very mechanistic physical model. We shall also explain how CO distributions based on these single pathway interference models can be modified by sprinkling (Copenhaver et al., 2002) additional non interfering COs to construct two-pathways models.

1.1. Single-pathway models

One way to mathematically incorporate the "repulsion" between COs is to force the probability density of distances separating two successive COs to have a particularly low value at small interval lengths. If one further takes the different intervals to be independent and identically distributed, one obtains a "Stationary Renewal Process" (SRP) framework (Zhao and Speed, 1996) for the formation of COs. Explicitly, one can think of the COs as being laid down from left to right on an axis that represents genetic position; for each new CO, say number i+1, one choses an interval length Δ_i giving the distance from the previous CO. The Δ_i are drawn independently from a given law $\rho(\Delta)$. All COs falling within the bivalent region are then kept as they are, the others are thrown away. Note that this procedure amounts to considering the centromere as just a "cold" region for recombination; interference then spans through the centromere within such a framework, as has been previously demonstrated experimentally (Colombo and Jones, 1997). A common choice for ρ is the gamma distribution

$$\Gamma_{\alpha}^{\nu}(x) = C(\alpha,\nu)\, x^{(\nu-1)} e^{-\alpha x} \qquad \text{(Equation 1)}$$

where C is the normalization constant $\frac{\alpha^{\nu}}{(\nu-1)!}$, ν is referred to as the shape parameter, and α is the rate parameter. This specification of ρ corresponds to what is called the gamma *model* (Broman and Weber, 2000). Forcing the mean number of COs to be 2 per Morgan and per bivalent leads to $\alpha = 2\nu$ when x is measured in Morgan, and the mean distance between COs in the SRP (on an infinite bivalent)

is then necessarily 50 cM. For $\nu = 1$, the intervals are distributed following an exponential law which is what arises in the absence of interference. For $\nu > 1$ the intervals are distributed so that short distances between COs are rare compared to the $\nu = 1$ case, *i.e*. one has positive interference. Interestingly, when ν is a positive integer, the gamma model is identical to the counting model of parameter $m = \nu - 1$ (McPeek and Speed, 1995). In this latter model, the interval between two successive COs is generated by adding $(m + 1)$ exponentially distributed variables. Since exponentially distributed distances correspond to the no interference case ($\nu = 1$), the counting model can also be viewed as first producing a collection of independent « precursors » (no interference) followed by a selection process in which every $(m + 1)$'th precursor is turned into a CO, and the others are discarded (NCOs) (Foss et al., 1993).

The gamma model is based on a statistical framework. Other approaches (King and Mortimer, 1990; Fujitani et al., 2002; Kleckner et al., 2004) are based on modeling some physical or chemical phenomena that might be involved in *mediating* interactions (interference) during CO formation. The best known of these is the BF model (Kleckner et al., 2004). That model is based on an analogy with an elastic film fused to a beam that is undergoing stretching. As the beam stretches and becomes longer, it produces a stress in the film which leads to cracks. A crack will release the film's stress in its immediate neighborhood. A crack that forms at one position makes it unlikely for another crack to form nearby, and thus cracks interfere with one another. If the cracks are considered to be CO points on the bivalent, one obtains a model for CO formation with interference. The implementation of this model is rather complex as some heterogeneities in the mechanical properties of the film must be introduced to yield crack precursors of various brittleness (see next paragraph). As the beam stretches, each precursor has a stress threshold beyond which it “cracks” (*i.e*. forms a CO). In the limit where the film is thin, a simple linear partial differential equation describes the state of the stress along the film. The important features to keep in mind are that (1) the stress at a crack vanishes; (2) the stress in the vicinity of the crack relaxes to its crack-independent value exponentially with distance; we denote the associated length scale by λ, so the stress in any interval containing no cracks can be written as $\sigma_0 + a e^{x/\lambda} + b e^{-x/\lambda}$. Furthermore, it is necessary to specify the stress at the end of chromosomes (Kleckner et al., 2004). For this we apply Neuman boundary conditions (Landau and Lifshitz, 1986) , which means that the stress at the ends of the film (bivalent) has zero derivative. The partial differential equation describing this system can be solved analytically with the general solution being of the form

$\sigma(x)=\sigma_0\left(1-\cosh\left(\frac{x-x_0}{\lambda}\right)\right)+B\sinh\left(\frac{x-x_0}{\lambda}\right)$ for the stress σ (*x*) at point *x* on one side of a crack positioned at x_0 (Kleckner et al., 2004). Note that there is a value *B* for each interval delimited by cracks or an edge of the chromosome. Each *B* must be adjusted so the boundary conditions are satisfied and σ (*x*)=0 at each crack. From this piecewise solution, one constructs an explicit formula for the stress at any given point given the set of cracks. In practice it is simpler to work with dimensionless quantities, so in our study λ is normalized by the SC length. Finally, to have the desired properties, the model must be adjusted: the maximum beam stretching is set so that one has the correct mean number of COs (twice the genetic length of the chromosome in Morgans) while λ is chosen so that the interference is of the desired strength. Note that very thin films correspond to small λ and thus to a very short interference range.

For the implementation of the BF model, we also follow the specification of Kleckner et al. (2004) for the precursors. These can be thought to correspond to DNA double strand breaks, some of which mature to COs. In the simulations of Kleckner et al. (2004), cf. their supplementary materials, they advocated taking the number of precursors to be 10 to 30 times the number of chiasmata. In practice, the model is relatively insensitive to this ratio, so we have set it to 20 in this work. Note that studies in maize (Franklin et al., 1999; Stack and Anderson, 2002) suggest values for this ratio ranging from 4 to 25, while the case of tomato leads to 17 (Stack and Anderson, 1986). These precursors are then positioned randomly on the bivalent. Furthermore, to each is assigned a random threshold according to the formula $\theta_i=1/\sqrt{x_i}$ where x_i is a random variable uniformly distributed in [0,1]. When the stress at a precursor exceeds this threshold, it turns into a crack. The model's intrinsic randomness leads to strong stochasticity in the determination of which precursors mature into COs. If on the contrary the stress on a precursor never exceeds its threshold, it is considered to lead to conversion and thus is not considered in this study of COs.

1.2. Connecting coordinates in physical SC and genetic space

The distances measured along the SC in the maize Late recombination Nodule (LN) data set are in micrometers. It is known that for maize, SC μm distances are roughly proportional to distances measured in base pairs giving about 6500 kbp per μm SC in euchromatin and ~9200 kbp per μm SC in heterochromatin, but these SC distances are not proportional to genetic distances (Anderson et al., 2003, 2006). Since the gamma model is formulated using genetic distances, it is necessary to convert

between physical SC (μm) and genetic (cM) distance spaces. However in practice, all SC positions and distances are taken relative to the total SC length, and thus lie between zero and one. To map the positions x_{SC} to genetic ones, we first build the density $\rho_{SC}(x_{SC})$, using all the COs of the data set for the chromosome considered. Then if a particular position on the chromosome has the coordinate x_{SC} in SC space, its coordinate x_G in genetic space is given by $2x_G = \int_0^{x_{SC}} \rho_{SC}(X)\,dX$.

Considering now the BF model, its motivation is based on physical space; however the model has no information regarding cold and hot regions of recombination. As a consequence, the CO positions generated by this model cannot be identified with physical coordinates. Furthermore, they cannot be identified with genetic coordinates either, as we demonstrate in Supplemental Figure 11. There we show the density of COs for a chromosome size given by that of maize chromosome 1. (We used the BF model with λ set to 0.2.) By definition of genetic space, CO density must be uniform, and it is not in the BF model. Positions generated in the BF model then correspond to a third space which we call IRD for "Interference Relevant Distance" space (Falque et al., 2007), and again a conversion must be implemented. Following the previous method for converting to genetic coordinates and letting $\rho_{IRD}(x_{IRD})$ be the density of COs in IRD space, we have $2x_G = \int_0^{x_{IRD}} \rho_{IRD}(X)\,dX$.

To derive this equation and the previous one, we assumed that the bivalent starts at $x = 0$ in all coordinate systems, and we have used the fact that $\rho_G(x_G) = 2$, corresponding to having on average two COs per Morgan on a bivalent. Explicitly, we determine ρ_{SC} using all the COs present in the data set and their positions, ordering them, and then assigning CO number j the position in genetic space $\frac{x_G}{L_G} = \frac{j}{K}$ where K is the total number of COs in the data set. If N is the total number of SCs in the data set, using the relation $2L_G = \frac{K}{N}$, we obtain $x_G(j) = \frac{j}{2N}$. The same procedure is used for IRD. Then for an arbitrary position x_{SC}, we use linear interpolation to find its x_G. These mappings can then be inverted, allowing us to translate from any space to any other. (Naturally, to compute a distance in any of these spaces, one computes the two coordinates in that space and takes their difference.) For the purpose of analyzing CO data sets, using either the gamma or the BF model, we transform the SC positions to genetic space and perform our fits there. This choice has the advantage that heterogeneity in CO rates is explicitly taken care of, and so our histograms (which require binning the data) contain more information than if one were to work in SC space directly.

1.3 Two-pathways models

In two-pathways models, pathway 1 (denoted P1) is subject to relatively strong interference, and pathway 2 (denoted P2) has insignificant or low levels of interference. Following previous work (Copenhaver et al., 2002), we model the presence of this second pathway by taking it to be independent of the first and without interference. The COs are thus obtained by taking the sum of the COs produced in each pathway. Clearly one can superpose in this fashion any two pathways, but in practice the second pathway has always been taken to be the No-Interference one, corresponding to the gamma model with $\nu = 1$. Since in nearly all organisms considered to date the second pathway produces fewer COs than the first, most authors refer to this approach as a « sprinkling » of the second pathway on top of the first. In our analysis, we used either the gamma model or the BF model for the first pathway. Let p be the average fraction of COs coming from the non-interfering pathway. To simulate CO formation in the two-pathways model, one first generates CO positions using P1, of given interference parameter (ν for the gamma model, λ for the BF model), using a genetic length of $(1-p)\ L_G$ where L_G is the genetic length of the chromosome of interest. Second, one generates CO positions with P2 using a genetic length of $p\ L_G$; then the fusion of the two lists of COs gives the desired result, enforcing the total genetic length of the chromosome. Hereafter the gamma (respectively BF) model with sprinkling of non-interfering P2 COs will be referred to as the GS (respectively BFS) model.

2. Inferring the best parameters

2.1. Fitting

In the *specification* of the models, some parameters must be « set ». For instance one wants to enforce a known genetic length for the chromosome of interest and one wants a fraction p of the COs to proceed via P2. A second task is to *adjust* the model's parameters by fitting to experimental data. For our purposes, the two-pathways models require fitting simultaneously p and the interference strength (ν for the gamma model and λ for the BF model). We discuss all these issues here.

Consider first the specification problem of ensuring a given genetic length L_G for a given pathway. In our implementation, we have chosen the convention for units whereby the coordinate x in IRD space spans the unit interval [0,1]. First, suppose that the P1 COs are produced within the gamma model. Since Equation 1 leads to a density of COs equal to α / ν, we see that one must set $\alpha = 2\ \nu\ L_G$ for a chromosome of genetic length L_G *for that pathway*. This rule applies in particular to the non-interfering

pathway: indeed the No-Interference model corresponds to $\nu = 1$ in the gamma model family. Thus if p is the fraction allocated to pathway P2 and L_{tot} is the total genetic length with *both* pathways contributing, we set $\alpha_{P1} = (1 - p)\ 2\ \nu\ L_{tot}$ and $\alpha_{P2} = p\ 2\ L_{tot}$; we also see that for the specification problem, p is simply set to its desired value. All this follows from the fact that IRD coordinates are just L_{tot} times smaller that genetic ones. Second, consider the case where the pathway P1 is described by the BF model. In this situation, no analytical calculation *a priori* ensures a given mean number of COs and we must resort to simulation. In this approach, we use the fact that we can determine quite accurately the mean number of COs produced for any given value of the maximum beam stress, using, for instance, 10^6 simulated meioses. (This sample size provides approximately a relative precision on the genetic length of 0.1% which is sufficient for our purposes.) Then the value of the maximum beam stress can be adjusted using a dichotomy search so that the correct genetic length (or half the mean number of COs per meiosis) is obtained. Since simulating CO formation is computationally very expensive in the BF model, we have introduced an efficient numerical procedure to search for the optimum value of the maximum stress parameter. Essentially, we exploit the monotonic behavior of the number of COs as a function of the value of the maximum beam stress. For each bivalent we determine how its number of COs increases with the stress parameter, and then we do a dichotomy search without having to perform new simulations for each value of the maximum beam stress.

Next, it is necessary to explain how we fit each model to the data, from which we shall extract the fraction p and the interference strength parameter that best adjusts the model to the data. In the single-pathway models, there is a single parameter to infer, while in the two-pathways models we must adjust both the interference parameter in P1 and the fraction p of COs from the non-interfering P2 pathway. In the case where P1 is described by the gamma model, the situation is rather ideal because one can compute the likelihood of the data given the model parameters. This then allows one to estimate the values of the parameters by maximizing this likelihood. Consider first the case $p = 0$. The CO positions of an experimental bivalent are converted into genetic positions in cM (genetic space), and then the bivalent's likelihood is computed as follows. Each inter-CO interval contributes the term of Equation 1 to the likelihood, and the product of these terms must be multiplied by two “end” contributions: one to go from the left end of the chromosome to the first CO, and one for going from the last CO to the right end of the chromosome. The formulas for these different terms have been given by Broman and Weber (2000); they even generalize the calculation to gametes instead of bivalents, but this generalization is not necessary here. Second, suppose now $p \neq 0$; the calculation begins by decomposing the

bivalent's COs into all possible ways of assigning COs to either pathway. If there are *k* COs , one has to produce 2^k assignments. For each assignment, one has a first list of COs coming from P1 and a second list for those coming from P2. For each list, one computes the likelihood as before for the COs to have formed in each pathway separately. The likelihood for one of these assignments is then the product of the two likelihoods, one coming from each pathway. Finally, the likelihood of the bivalent is obtained by summing the likelihoods obtained from the 2^k assignments. These formulas have been derived by Copenhaver et al. (2002).

Unfortunately, for complex models such as the BF, it is not possible to compute the likelihood of having a given list of CO positions on a bivalent. We have thus resorted to « projected likelihood » methods. Instead of finding the actual likelihood of a list of CO positions, we consider a low dimensional projection of the data and work with the likelihood of the projection. This is done as follows. From the full list of CO positions, we first construct a derived (projected) quantity (hereafter referred to as an observable). In general this observable is a real number. We then use simulations to determine the distribution of this observable as predicted by the model, with one distribution for each setting of the model's different parameter values. From the distribution, we can compute the likelihood of the projected experimental data for all desired parameter values. Maximizing this (projected) likelihood gives the inference of the parameter values.

A simple example of such a projection is obtained if one ignores the positions of the COs and considers only the number of COs in a bivalent. This observable has been used in the past but it is not very discriminating for the strength of interference (Broman and Weber, 2000). More powerful for interference analysis is the distribution of distances between successive COs for bivalents having 2 COs. This can be exploited in a projected likelihood approach as follows: let P(0), P(1), P(2), ... be the probability in the model of obtaining 0, 1, 2, ... COs and let ρ_2 be the probability density of inter-CO distances for bivalents with exactly 2 COs. The projected likelihood of a bivalent with *k* COs will then be P(*k*) if $k \neq 2$ and $P(2)\rho_2(\Delta)$ if *k*=2, where Δ is the distance between the two COs. We find that this approach improves the power of the inference method compared to using only P(0), P(1), P(2), ..., but not sufficiently compared to the full likelihood when it is available (as in the GS model). Thus to do better and obtain an inference procedure that is not much less powerful than a full likelihood approach, we have implemented a fitting procedure based on assigning a score that takes into account CO intervals for *all* bivalents. The score should be designed so that data having statistical properties similar to the model will have high scores. Since inter-CO distances are particularly relevant for

interference, we have defined our Projected Likelihood Score (PLS) as follows:

$PLS = P(0)$ $(respectively\ P(1))$ for bivalents with 0 (respectively 1) CO

$PLS = P(k)\sum_{i=1}^{k-1} \rho_k(\Delta_i)$ for bivalents with $k > 1$ COs

where Δ_i is the i'th interval length (between CO i and CO i+1) and ρ_k is the density of these lengths for bivalents with k COs. For all these values of k, one has simply to determine the different ρ_k given the model and its parameter settings.

One can use simulations to measure the reliability of any of these fitting procedures. Using simulated data produced within a model, it is easy to determine to what extent one recovers the parameters by the different fitting approaches, and also quantify the uncertainty in these parameters.

The actual fitting to infer the "best" parameter values can proceed by performing a scan of parameter space. When there is a single parameter to infer (single-pathway models), this is relatively efficient. However for the two-pathways models ($p \neq 0$), we find this to be too costly in computation time, so instead we perform "hill climbing" on the likelihood or score function. The hill climbing stops when no further improvement in the score is found. The associated parameters giving this peak score are then quoted as giving the best fit. An illustration of the "shape" of the hill to climb for the PLS score is given in Figure 4 of the article. We see it is relatively smooth, and importantly, has a single peak, justifying *a posteriori* the hill climbing for reaching the maximum score.

2.2. Confidence intervals on inferred parameters based on re-simulation

The inferred parameters are obtained from fitting procedures which go from maximum likelihood to using a score for quantifying the goodness of fit (as described in the previous section). Denote these inferred values by p^* and I^* (corresponding to ν^* for gamma, λ^* for BF). To derive their 95% confidence intervals, we follow Viswanath and Housworth (2005) and proceed as follows. First we produce by simulation 1000 artificial data sets. Each such data set consists of N meiotic SCs obtained by simulating the model of interest (e.g., BFS) using p^* and I^*. N here is the number of SCs in the actual experimental data set of interest, and thus N changes slightly from chromosome to chromosome. Second, for each such artificial data set, we run our fitting procedure which produces one pair of inferred parameters (p, I). (In the single-pathway models, p is of course set to 0.) The list of these 1000 re-simulated parameter values gives us an approximation to the distribution of each inferred parameter. For both p and I, extracting the associated 95% confidence interval is then straightforward, one just has

to find the tails containing 2.5% of the distribution. Note that because this approach requires repeating the fitting procedures many times, it dominates the computation time required by our analyses.

REFERENCES

Anderson, L.K., Doyle, G.G., Brigham, B., Carter, J., Hooker, K.D., Lai, A., Rice, M., and Stack, S.M. (2003). High-Resolution Crossover Maps for Each Bivalent of Zea mays Using Recombination Nodules. Genetics **165:** 849-865.

Anderson, L.K., Lai, A., Stack, S.M., Rizzon, C., and Gaut, B.S. (2006). Uneven distribution of expressed sequence tag loci on maize pachytene chromosomes. Genome Research **115:** 115-122.

Broman, K.W., and Weber, J.L. (2000). Characterization of Human Crossover Interference. The American Journal of Human Genetics **66:** 1911-1926.

Colombo, P.C., and Jones, G.H. (1997). Chiasma interference is blind to centromeres. Heredity **79:** 214-227.

Copenhaver, G.P., Housworth, E.A., and Stahl, F.W. (2002). Crossover Interference in Arabidopsis. Genetics **160:** 1631-1639.

Falque, M., Mercier, R., Mézard, C., de Vienne, D., and Martin, O.C. (2007). Patterns of Recombination and MLH1 Foci Density Along Mouse Chromosomes: Modeling Effects of Interference and Obligate Chiasma. Genetics. **176:** 1453-1467.

Foss, E., Lande, R., Stahl, F.W., and Steinberg, C.M. (1993). Chiasma Interference as a Function of Genetic Distance. Genetics **133:** 681-691.

Franklin, A.E., McElver, J., Sunjevaric, I., Rothstein, R., Bowen, B., and Cande, W.Z. (1999). Three-Dimensional Microscopy of the Rad51 Recombination Protein during Meiotic Prophase. Plant Cell **11:** 809-824.

Fujitani, Y., Mori, S., and Kobayashi, I. (2002). A Reaction-Diffusion Model for Interference in Meiotic Crossing Over. Genetics **161:** 365-372.

King, J.S., and Mortimer, R.K. (1990). A Polymerization Model of Chiasma Interference and Corresponding Computer Simulation. Genetics **126:** 1127-1138.

Kleckner, N., Zickler, D., Jones, G.H., Dekker, J., Padmore, R., Henle, J., and Hutchinson, J. (2004). A mechanical basis for chromosome function. Proc Natl Acad Sci U S A. **101:** 12592-12597.

Landau, L.D., and Lifshitz, E.M. (1986). Theory of Elasticity: Course of Theoretical Physics: 7. (New-York: Pergamon).

McPeek, M.S., and Speed, T.P. (1995). Modeling Interference in Genetic Recombination. Genetics **139:** 1031-1044.

Stack, S.M., and Anderson, L.K. (2002). Crossing over as assessed by late recombination nodules is

related to the pattern of synapsis and the distribution of early recombination nodules in maize. Chromosome Research **10:** 329-345.

Stack, S.M., and Anderson, L.K. (1986). Two-dimensional spreads of synaptonemal complexes from solanaceous plants. Chromosoma **94:** 253-258.

Viswanath, L., and Housworth, E. (2005). InterferenceAnalyzer: Tools for the analysis and simulation of multi-locus genetic data. BMC Bioinformatics **6:** 297.

Zhao, H., and Speed, T.P. (1996). On Genetic Map Functions. Genetics **142:** 1369-1377.